Toward potent antibiofilm degradable medical devices: A generic method for the antibacterial surface modification of polylactide

Sarah El Habnouni, Jean-Philippe Lavigne, Vincent Darcos, Barbara Porsio, Xavier Garric, Jean Coudane, Benjamin Nottelet

▶ **To cite this version:**

Sarah El Habnouni, Jean-Philippe Lavigne, Vincent Darcos, Barbara Porsio, Xavier Garric, et al.. Toward potent antibiofilm degradable medical devices: A generic method for the antibacterial surface modification of polylactide. Acta Biomaterialia, 2013, 9 (8), pp.7709-7718. 10.1016/j.actbio.2013.04.018 . hal-00958350

HAL Id: hal-00958350
https://hal.science/hal-00958350

Submitted on 22 Jan 2024

HAL is a multi-disciplinary open access archive for the deposit and dissemination of scientific research documents, whether they are published or not. The documents may come from teaching and research institutions in France or abroad, or from public or private research centers.

L'archive ouverte pluridisciplinaire **HAL**, est destinée au dépôt et à la diffusion de documents scientifiques de niveau recherche, publiés ou non, émanant des établissements d'enseignement et de recherche français ou étrangers, des laboratoires publics ou privés.

Distributed under a Creative Commons Attribution - NonCommercial - NoDerivatives 4.0 International License

Toward potent antibiofilm degradable medical devices: A generic method for the antibacterial surface modification of polylactide

Sarah El Habnouni [a], Jean-Philippe Lavigne [b], Vincent Darcos [a], Barbara Porsio [a], Xavier Garric [a], Jean Coudane [a], Benjamin Nottelet [a,*]

[a] *Institut des Biomolécules Max Mousseron (IBMM), Artificial Biopolymers Group, UMR CNRS 5247, University of Montpellier 1, University of Montpellier 2, Faculty of Pharmacy, 15 Av. C. Flahault, Montpellier 34093, France*
[b] *Bacterial Virulence and Infectious Disease, INSERM U1047, University of Montpellier 1, UFR Médecine Site de Nîmes, 186 Chemin du Carreau de Lanes, CS 83021, 30908 Nîmes Cedex 2, France*

A B S T R A C T

The effects of biomaterials on their environment must be carefully modulated in most biomedical applications. Among other approaches, this modulation can be obtained through the modification of the biomaterial surface. This paper proposes a simple and versatile strategy to produce non-leaching antibacterial polylactide (PLA) surfaces without any degradation of the polyester chains. The method is based on a one-pot procedure that provides a ''clickable'' PLA surface via anionic activation which is then functionalized with an antibacterial quaternized poly(2-(dimethylamino)ethyl methacrylate) (QPDMAEMA) by covalent immobilization on the surface. The anti-adherence and antibiofilm activities of modified PLA surfaces are assessed for different QPDMAEMA molecular weights and different quaternization agents. Antibacterial PLA surfaces are shown to be very active against Gram-negative and Gram-positive strains, with adherence reduction factors superior to 99.999% and a marked reduction in biofilm on the most potent surfaces. In addition to this substantial antibacterial activity, the proposed PLA surfaces are also cytocompatible, as demonstrated through the proliferation of L929 fibroblasts.

1. Introduction

Modulating and controlling the surface properties of biomaterials is of crucial importance in biomedical applications and, although generally studied in solution for reasons of simplicity, the importance of specific surface reactions and interactions has widely been recognized [1]. Ideally, implantable biomaterials, whether degradable or not, should induce a minimal inflammatory response, promote vascular and fibroblastic colonization, limit the risk of infection, and promote integration with surrounding tissues [2,3]. This, however, is far from being the case with biomaterials used for implants as they are prone to serious bacterial infections. For example, polylactide (PLA) medical devices such as screws and pins for orthopedic and trauma surgery present a 4% infection rate [4]. More generally, clinical studies have highlighted the fact that depending on their type, 10–50% of implants are infected at some point in their lifecycle and that bacteria are found in approximately 90% of all implantation sites immediately after surgery [5]. Among other problems, these post-operative nosocomial infections can delay healing. Because prosthesis-related infections may cause severe complications weeks to years after implantation, and ultimately require removal of the prosthetic material [6], the conventional procedure is to administer intravenous antibiotics intra-operatively, possibly followed by post-operative systemic antibiotic therapy. Unfortunately, these measures may fail, especially if a biofilm has formed on the surface of the implant. Many reviews have focused on biofilm formation and readers are invited to refer to these for an in-depth description of the mechanisms involved [7–9].

To avoid the formation of biofilm, an attractive alternative and/or complement to antibiotic treatment is to use biomaterials that possess antibacterial surfaces. This is particularly the case for aliphatic polyester-based materials that today are widely used clinically. Various strategies have been developed to produce these materials and rely on two different approaches: the non-covalent and covalent immobilization of antibacterial agents. The first approach includes drug-releasing coatings [10,11] and mixing techniques [12–14] but intrinsically leads to loss of activity after drug elution and the risk of promoting the emergence of multi-drug-resistant bacteria. The second approach includes plasma treatment [15,16], photo-grafting [17] and chemical modification by aminolysis or hydrolysis [18–21]. These techniques have been widely employed for the purposes of modifying polymer surfaces, including polyesters. They nevertheless run into two main problems. The first is due to the nature of the degradable aliphatic

* Corresponding author. Fax: +33 (0)4 67 52 08 98.
E-mail address: benjamin.nottelet@univ-montp1.fr (B. Nottelet).

polyesters that cannot be modified without considering their relative fragility, especially in cases of aminolysis or hydrolysis. The second is that the surface modification in most cases is not designed to provide a stable, shelf-ready, general platform for specific post-functionalization. In this context, and based on our experience with the modification of poly(ε-caprolactone) (PCL) [22–24], we recently reported a mild and versatile chemical modification strategy for PLA surfaces. By combining controlled anionic surface activation and a subsequent one-pot nucleophilic substitution we produced clickable PLA surfaces bearing propargyl groups [25]. In this present paper, we demonstrate the versatility of this approach by describing the production of antibacterial PLA surfaces functionalized with various quaternized poly(2-(dimethylamino)ethyl methacrylate) (QPDMAEMA).

A number of features common to many polycations, including polyquaternary ammoniums (PQAs), are thought to explain their antibacterial activity. These include interactions between polymer cations and the negatively charged outer membranes, cell walls and even cytoplasmic membranes of bacteria [26–28]. One advantage of this cell lysis mechanism is that PQAs are biocidal for a broad spectrum of pathogenic microorganisms and as such have been used for many surface modifications. Without being exhaustive, Supplementary Information Table S1 gives examples of biomaterial surfaces that have been associated with PQA antibacterial polymers. For a more complete overview, readers are invited to refer to recent reviews [16,29,30]. As can be seen, most studies have focused on inorganic surfaces or non-degradable polymer surfaces. This is due to the difficulty of activating the surface of aliphatic polyesters without degradation. As a consequence, and to the best of our knowledge—besides our recent work—only one example of polyester surfaces being modified for antibacterial purposes by the direct immobilization of PQAs has been described, by Gutierrez-Villarreal et al., based on the UV-photografting of poly(*N*-vinylpyrrolidone)/iodine complexes onto PLA films [31]. However, the approach adopted by Xu et al. should also be noted; this is based on the surface-initiated atom transfer radical polymerization of glycidyl methacrylate or methacrylic acid on PLA or PCL surfaces, functionalized with an atom transfer radical polymerization (ATRP) initiator [20,21]. Although not used for antibacterial applications, this "grafting from" strategy may be of interest for the development of degradable antibacterial materials. However, as it is based on surface aminolysis or hydrolysis, this strategy may cause a problem of polymer degradation, and thus the production of short polymer chains that are released from the surface, resulting in modified surface properties and morphology.

In the work described herein, we prepared a PLA clickable surface by controlled anionic activation that did not cause any degradation of the polymer surface material. These stable, shelf-ready PLA surfaces may then be functionalized by a "grafting to" approach using QPDMAEMAs of various molecular weights (MWs), and alkylating agents. The anti-adherence, biocidal and antibiofilm activity of the PLA antibacterial surface bearing various QPDMAEMAs was also assessed against four bacterial strains. Advantageously, the strategy proposed herein can be used to modulate antibacterial activity by grafting pre-synthesized, controlled PQAs. Finally, the cytocompatibilty of the best candidate was evaluated by a proliferation study using murine L929 fibroblasts.

2. Materials and methods

2.1. Materials

PLA_{94} was synthesized by bulk ring-opening copolymerization of L-lactide (88%) and DL-lactide (12%) (PURAC, Lyon, France), using tin 2-ethylhexanoate as catalyst ($\bar{M}_n = 100000$ g mol^{-1}; Đ = 1.9). PLA_{94} plates were shaped using a hydraulic heated press (Carver 4120-289). The plates were heated at 130 °C and PLA powder was pressed for 5 min before cooling under pressure (1.5×10^7 Pa). PLA_{94} plates 500 μm thick were obtained. *N*,*N*-Dimethylamino-2-ethyl methacrylate (DMAEMA, 98%, Aldrich, St Quentin Fallavier, France) was passed through a column of basic alumina to remove stabilizing agents. Toluene (Aldrich) and dichloromethane (Aldrich) were dried by refluxing over CaH_2 and distilled before use. Triethylamine (TEA, Aldrich) was distilled over KOH. Tetrahydrofuran (THF, Aldrich) was dried by refluxing over a benzophenone–sodium mixture until a deep blue colour was obtained, and was then distilled. PrestoBlue™, modified Eagle's medium (MEM), horse serum, penicillin, streptomycin, Glutamax, and Dulbecco's phosphate-buffered saline (DBPS) were purchased from Invitrogen (Cergy Pontoise, France). Cellstar® polystyrene tissue culture plates (TCPS) were purchased from Greiner Bio-One (Courtaboeuf, France).

All other solvents and chemicals were purchased from Aldrich and were used as received.

2.2. Methods

2.2.1. Synthesis of clickable PLA surfaces

Clickable PLA surfaces were prepared in accordance with a recently described procedure [25]. Typically, a PLA_{94} plate (mass = 125 mg, thickness = 500 μm, area = 1.76 cm^2) was immersed in a stirred solution of 2.0 M lithium diisopropyl amide (LDA) (1.5 ml, 3 mmol) in anhydrous tetrahydrofuran (60 ml)/ethyl ether (120 ml) at −50 °C in an argon inert atmosphere. This activation step lasted 30 min before propargyl bromide (700 μl, 6 mmol) was added at −30 °C. The mixture was stirred for 1 h at −30 °C and then raised to room temperature. The PLA plate was quenched and washed with water, diethyl ether and methanol. Residual solvents were removed under vacuum.

2.2.2. Synthesis of well-defined quaternized and clickable PDMAEMA (α-N_3-QPDMAEMA)

Clickable PDMAEMAs of controlled MWs were synthesized by ATRP. The (3-azidopropyl)bromoisobutyrate initiator was synthesized in accordance with a previously described procedure (Supplementary Information, Scheme S1) [32]. In a typical experiment, polymerization was carried out using the standard Schlenk technique in an argon atmosphere. CuBr (118 mg, 0.82 mmol, 1 equiv.) and the initiator (206 mg, 0.82 mmol, 1 equiv.) were placed in an oven-dried Schlenk tube fitted with a rubber septum. Degassed toluene (7 ml) and DMAEMA (7 ml, 41.5 mmol, 50 equiv.) were transferred to the tube via a degassed syringe. The solution was further degassed by three freeze–thaw–pump cycles. The mixture was stirred rapidly under argon and *N*,*N*',*N*'',*N*''-pentamethyldiethylenetriamine (PMDETA) was added. The resulting mixture was placed in a temperature-controlled oil bath at 60 °C for 20 min. The reaction was stopped by immersion in liquid nitrogen, and the catalyst was removed by passing through a column of activated basic alumina prior to MW analysis. Conversion was measured by ^{1}H nuclear magnetic resonance spectroscopy (NMR).

^{1}H NMR (300 MHz, $CDCl_3$) δ (ppm): 3.98 (CH_2OC=O), 3.33 (CH_2N_3), 2.49 (CH_2N), 2.21 (N(CH_3)$_2$), 1.6–2.0 (CH_2C(CH_3)C=O), 0.65–1.11 (CH$_2$C(CH_3)C=O).

PDMAEMA polymers were then further quaternized. In a typical experiment, α-azido PDMAEMA (500 mg) was dissolved in THF (100 ml) in a round-bottom flask. The mixture was stirred and an excess (2 equiv.) of quaternizing agent (heptyl iodide or methyl iodide) was added. The solution was stirred at room temperature overnight. Crude copolymer was then purified by dialysis against

deionized water. The final aqueous solution was freeze-dried to yield the quaternized α-azido PDMAEMA.

2.2.3. Immobilization of α-N_3-QPDMAEMA on PLA surfaces

α-azido QPDMAEMA (100 mg, 0.6 mmol) was dissolved in a mixture of water (1 ml)/ethanol (3 ml) and a clickable PLA plate was immersed in the solution. Cu^I catalyst was then generated in situ using copper sulfate (300 μl of a 1 M aqueous solution) and sodium ascorbate (600 μl of a 1 M solution). The reaction was performed at 40 °C for 2 days. The PLA plate was then extensively washed by dialysis against water until no fluorescence was detected in the dialysis medium. The plate was then rinsed with ethanol and methanol, and was finally dried under vacuum prior to analysis. Its surface was analyzed by X-ray photoelectron spectrometry (XPS). Size exclusion chromatography (SEC) analyses were performed using refractometric and fluorescence double detection after dissolving the surface in THF.

2.2.4. Characterization of polymers and surfaces

2.2.4.1. NMR. ^{1}H NMR and ^{13}C NMR spectra were recorded on a Bruker spectrometer (AMX300) operating at 300 and 75 MHz, respectively. Deuterated chloroform or deuterated dimethyl sulfoxide were used as solvents. Chemical shifts were expressed in ppm with respect to tetramethylsilane (TMS).

2.2.4.2. ATR-FTIR spectroscopy. Fourier transform infrared (FTIR) spectra were recorded on a Perkin Elmer Spectrum 100 FT-IR spectrometer using the attenuated total reflectance (ATR) method.

2.2.4.3. Size exclusion chromatography. SEC was performed at room temperature on a Waters system equipped with a guard column, a 600 mm PLgel 5 mm Mixed C column (Polymer Laboratories), a Waters 410 refractometric detector and a Waters 470 scanning fluorescence detector. Calibration was established with poly(styrene) standards from Polymer Laboratories. THF and THF/TEA (95/5; v/v) for PDMAEMA analyses were used as eluent at a flow rate of 1 ml min^{-1}.

2.2.4.4. X-ray photoelectron spectrometry. XPS spectra were obtained on an ESCALAB 250 Photoelectron Spectrometer with Al K_α radiation (1486.6 eV) and overall instrument resolution of 1.1 eV. All spectra were collected at an electron take-off angle of 90° to the sample surface. 400 μm^2 of each surface were analyzed. The binding energies were corrected by referencing the binding energy of the C–C component of C 1*s* to 284.8 eV.

2.2.4.5. Atomic force microscopy (AFM). AFM studies were carried out on a Nanoman atomic force microscope (Veeco Metrology, Santa Barbara, CA) equipped with a closed loop and run by Nanoscope 5 software (Bruker Instrument). Images were acquired in tapping mode under ambient conditions with an NCL cantilever (Nanosensors, Neuchatel, Switzerland) at a resonance frequency of around 150 kHz. The needle AFM probe was conical with a radius at the apex of 5 nm (maximum). Sampling was set at 512 pixels and 512 lines. Images were analyzed by Gwyddion 2.26 software (http://gwyddion.net/) and roughness is given as root mean square (rms).

2.2.5. Bacterial strains

Four clinical bacterial strains in the early stationary phase were used: *Escherichia coli* NECS19923, *Staphylococcus aureus* NSA4201, *S. epidermidis* NSE175861 and *Pseudomonas aeruginosa* NPA01. NECS19923 strain was genetically modified to express green fluorescent protein (GFP) using a pBBR-derived non-mobilizable plasmid carrying a GFP expression cassette.

2.2.6. Anti-adherence activity

Before conducting any in vitro antibacterial tests, the bacterial strains were first grown aerobically overnight on Muller Hinton medium at 37 °C with stirring. Bacterial adherence to modified plates was assessed in accordance with a previously described procedure [33]. The PLA plates were immersed in a bacterial solution (OD_{600} = 0.05) for 1 h, then non-adherent bacteria on the sample surface were removed by repeated washings with sterilized water. The plates were then incubated in neutral medium for 24 h at 37 °C under static conditions. PLA plates were rinsed in sterile saline to remove any non-biofilm population cells that may have deposited on the samples, then transferred to 2 ml saline (suspension A) and vortexed vigorously for 30 s. The samples were then transferred to 2 ml sterile saline (suspension B) and sonicated for 3 min. Samples were transferred once more to 2 ml sterile saline (suspension C) and vortexed vigorously for 30 s. Suspensions A, B and C were pooled, serially diluted and plated onto Luria agar for viable counting. The cells removed during these three phases represent the loosely attached biofilm population. Following the final vortex step, the samples were blotted onto the surface of a pre-dried Mueller Hinton agar plate for 1 min. The process was repeated through a succession of 15 pre-dried plates and colony counts were performed, following an overnight incubation at 37 °C. Finally, total bacterial adherence was calculated by adding the colony forming unit (CFU) count after overnight incubation of the agar plates at 37 °C, to all cultivated bacteria.

Bacteria on the surface of the PLA plates were visualized by immersing the plates in a dilute culture solution of *E. coli gfp+*(OD_{600} = 0.05, i.e. $\sim 1 \times 10^5$ CFU ml^{-1}) in accordance with the procedure described previously. After 1 h, the plates were washed with sterilized water to remove non-adherent bacteria and examined under a Leica fluorescence microscope. All these tests were performed in triplicate.

2.2.7. Bactericidal activity

Bactericidal activity was assessed by Live/Dead assay. The PLA plates were immersed in a bacterial solution (OD_{600} = 0.05, i.e. $\sim 1 \times 10^5$ CFU ml^{-1}) for 1 h, then non-adherent bacteria on the sample surface were removed by repeated washings with sterilized water. The plates were then incubated in neutral medium for 24 h at 37 °C under static conditions before being washed three times with deionized water. The plates were then immersed in 2 ml Live/Dead BacLight® solution (Invitrogen®) for 20 min at room temperature in the dark. After rinsing with PBS, the plates were placed between a slide and coverglass with moviol and examined under a fluorescence microscope (×20 and ×100). All these tests were performed in triplicate.

2.2.8. Biofilm formation

The susceptibility of the modified PLA plates to biofilm formation was evaluated by creating a liquid–air interface between the plate and a bacterial suspension (OD_{600} = 0.05, i.e. $\sim 1 \times 10^5$ CFU ml^{-1}). To do this, the different plates were placed vertically in a 12-well Greiner plate containing 2 ml of Muller–Hinton growth medium, and 20 μl of cell suspension in PBS were added. After incubating under static conditions for 16 h at 37 °C in a 100% humidity atmosphere, unattached bacteria were removed from the plates by repeated washings with sterilized water. A biofilm formed under these conditions on the bare plates, at the liquid–air interface. Biofilm-forming bacteria were recovered by immersion in dimethyl sulfoxide (DMSO) and 250 μl of this DMSO-containing bacterial solution were analyzed in a Mithras LB940 luminometer (Berthold). Biofilm formation was expressed in relative luminescence units (RLU). Alternatively, biofilm formation was evaluated by examination under a fluorescence microscope. In this case, after rinsing with PBS, the plates were placed

between a slide and cover glass with moviol and examined under a Leica fluorescence microscope (×20 and ×100). All these tests were performed in triplicate.

2.2.9. Cytocompatibility

Mouse L929 fibroblasts (L929) were cultured in modified Eagle's medium (MEM) containing 10% horse serum, penicillin (100 μg ml^{-1}), streptomycin (100 μg ml^{-1}) and Glutamax (1%). The PLA plates were disinfected in ethanol for 30 min before being immersed in a solution of sterile PBS containing penicillin and streptomycin (1 mg ml^{-1}) and incubated for 48 h at 37 °C. The plates were then rinsed three times with sterile PBS before being soaked for 12 h in sterile PBS. These sterile PLA plates were stamped to fit the wells of 24-well cell culture plates. In vitro cytocompatibility was assessed by monitoring the proliferation of L929 fibroblasts on the surface of the plates. To do this, the plates were placed in polystyrene 24-well tissue culture plates (TCPS) and seeded with 1×10^4 L929 cells. Cell viability after 1, 2 and 3 days was evaluated using the PrestoBlue™ assay, which reflects the number of living cells present on a surface at a given time point. Culture medium was removed at scheduled time points and replaced by 1 ml of fresh medium containing 10% PrestoBlue™. Fluorescence at 530 nm (excitation) and 615 nm (emission) was measured on a Victor X3 photometer (Perkin Elmer). All data points and standard deviations correspond to measurements in triplicate.

2.3. Data analysis

All data are expressed as means ± SD and correspond to measurements in triplicate.

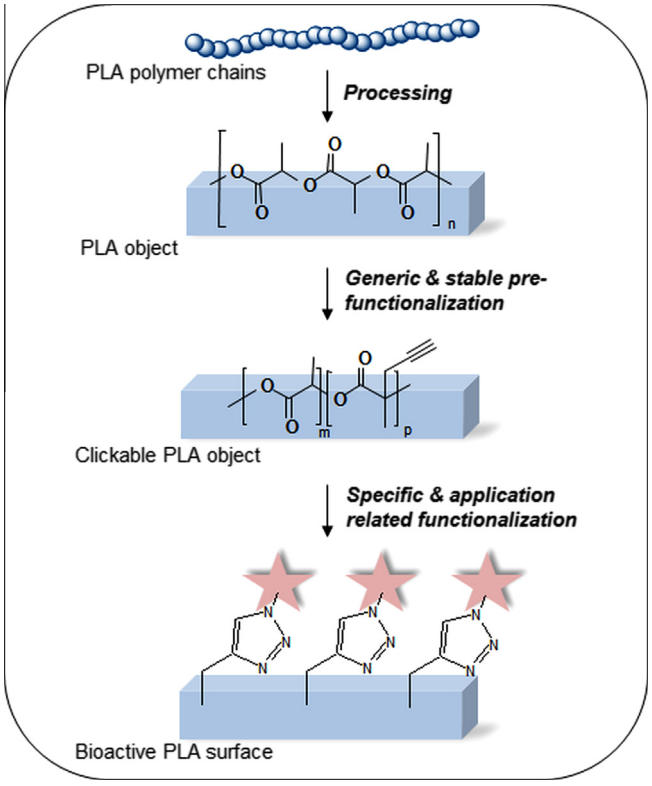

Scheme 1. General methodology for the preparation of PLA bioactive surfaces via combination of anionic activation and the "grafting onto" technique.

3. Results and discussion

3.1. Pre-functionalization of PLA surfaces

Our group recently reported on the possibility of functionalizing the surface of a three-dimensional PLA_{94} object by a three-step strategy that combines (i) synthesis of a propargyl-functionalized surface via anionic activation, (ii) synthesis of an azido-functionalized bioactive compound and (iii) Huisgen's 1,3-dipolar cycloaddition (click chemistry) of the bioactive compound to the propargylated surface (Scheme 1) [25]. The first critical step, i.e. the anionic activation of degradable PLA surfaces, requires careful control of reaction conditions to avoid any hydrolytic degradation of the polyester. Optimized mild conditions were determined in our previous work and were employed in the study described here. Briefly, PLA plates were functionalized using the non-nucleophilic strong base LDA in a solvent/non-solvent mixture of tetrahydrofuran/diethyl ether (1/2 v/v). This activation step was conducted for 30 min at a low temperature (−50 °C) to avoid PLA degradation and was followed by the addition of propargyl bromide. Finally, the plate was washed with water and diethyl ether to remove non-covalently grafted species. As the chemical modification takes place only at the very surface of the plates, classical penetrating characterization techniques (FTIR or Raman spectroscopies) are unable to detect any propargyl groups. However, as discussed in our previous report, the clickable fluorescent probe 9-azidomethylanthracene may be used to evaluate the functionalization and availability of the propargyl groups located on the PLA surface, and the possible degradation of PLA chains. This indirect detection technique was again used in the present study. Refractometric and fluorometric SEC analyses of the PLA surface evidenced fluorescent probe only at the surface of the material, with no fluorescence being detected in the core. This confirmed surface propargyl functionalization without bulk modification. This refractometric analysis also showed that no decrease had occurred in PLA MW as a result of the anionic activation reaction. Chromatograms of the PLA surface and core were similar, showing that no change had occurred in MW or dispersity ($\bar{M}_n$ = 100000 g mol^{-1}; Đ = 1.9) (Supplementary Information Fig. S1). Surface morphology was further characterized by AFM. Fig. 1a shows the surface of the neat PLA with very low roughness of only 3 nm (rms value). In comparison, the propargylated plate presents a greater, but still limited, roughness of 14 nm (Fig. 1b). Unsurprisingly, the anionic activation causes weak chemical etching on the PLA surface and it may be hypothesized that only a very small proportion of the polymer chains are hydrolyzed during anionic activation. These smaller chains are very likely washed away during the modification process, explaining the limited increase in surface roughness and the lack of any impact on overall PLA MW at the surface, as demonstrated by the SEC analyses. The specific conditions used in this study thus yield a stable clickable PLA surface. It should nevertheless be noted that this propargylated surface is obtained at the cost of slightly greater roughness, but without any decrease in MW and without altering the macroscopic 3-D shape of the plate (Supplementary Information Fig. S2). This last point is of crucial importance if this strategy is to be used to modify the surface prosthetic materials that have a defined shape (interference screws, surgical meshes, etc.).

3.2. Synthesis of well-defined α-N_3-QPDMAEMA

PQAs are well known for their antibacterial properties that may be explained by (i) their adsorption onto the bacterial cell surface driven by electrostatic interactions, (ii) their diffusion through the cell wall, driven by hydrophobic interactions, (iii) their adsorption onto the cytoplasmic membrane, and (iv) the disruption of the cytoplasmic membrane by the insertion of hydrophobic groups in

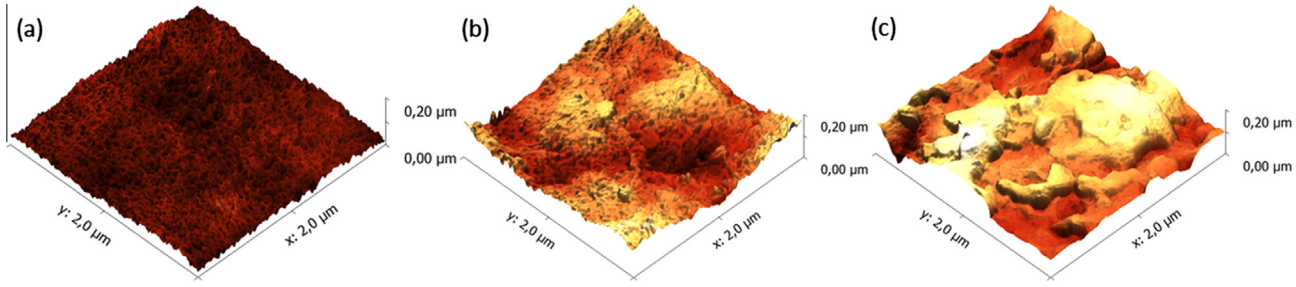

Fig. 1. AFM images of PLA surfaces (a) before modification, (b) after propargylation and (c) after functionalization with QPDMAEMA (8C7).

the cell membrane and/or the exchange of surface-bound polycations with divalent metal cations (Mg^{2+}, Ca^{2+}) in the cell membrane [26–28]. Of these PQAs, quaternized PDMAEMA derivatives (QPDMAEMAs) have been proposed and grafted onto non-degradable inorganic and organic substrates (Supplementary Information Table S1). Having demonstrated in a previous paper the feasibility of grafting a QPDMAEMA to a propargylated PLA surface, we focused in the study described herein on evaluating the impact of certain macromolecular parameters, including MW, on the antibacterial activity of QPDMAEMA-modified PLA surfaces. For this purpose, we synthesized a family of well-defined PDMAEMAs of various MWs by ATRP as this is known to provide a controlled polymerization of DMAEMA [34]. In particular, an azido-bromoester derivative was synthesized and used as an initiator to yield well-defined and clickable PDMAEMAs as described by Agut et al. (Supplementary Information Scheme S1) [32]. The polymerization was conducted at 60 °C in toluene for 20 min in the presence of CuBr/PMDETA, as catalytic system, and defined amounts of the initiator, to generate PDMAEMAs of controlled MWs. Molar mass and polydispersity were controlled under these experimental conditions, as confirmed by ^{1}H NMR calculations of molar masses and SEC analyses in THF/TEA (95/5, v/v) (Supplementary Information Fig. S3a and c). Chromatograms showed monomodal traces corresponding to $M_{n,SEC}$ ranging from 5000 to 10 000 g mol^{-1} and a polydispersity index of less than 1.2 (Table 1). Values for molar mass by SEC were determined relative to polystyrene standards. More accurate values were provided by ^{1}H NMR using the following equation:

$$M_{n,NMR} = I_e/I_a \times M_{DMAEMA} + M_{init}, \quad (1)$$

where I_a, I_e, M_{DMAEMA} and M_{init} are the intensity of methylene protons a in the end groups, the intensity of methylene protons e in the α-N_3-PDMAEMA main chain, the molar mass of the DMAEMA monomer unit, and the molar mass of the initiator, respectively. Accordingly, $M_{n,NMR}$ were calculated and were in good agreement with the theoretical values, thus confirming the controlled character of the ATRP of DMAEMA. Characteristic protons of α-N_3-PDMAEMA chain-end introduced by the functionalized initiator were accurately identified by ^{1}H NMR with a signal at 3.3 ppm corresponding to methylenic protons adjacent to the azido function [32]. Additionally, IR spectra clearly showed a band at 2100 cm^{-1} corresponding to this function (Supplementary Information Fig. S3b). Clear evidence was therefore available that the azido functions were highly conserved in this α-N_3-PDMAEMA. Finally, quaternized α-azido-PDMAEMA (α-N_3-QPDMAEMA) was obtained by a conventional technique using methyl iodide or heptyl iodide as alkylating agents in tetrahydrofuran for 18 h at room temperature. 85–90% quaternization was confirmed by ^{1}H NMR analyses on the basis of the intensity of the $-CH_2-N(CH_3)_2$ given by PDMAEMA at ~2.2–2.5 ppm, which decreased and was replaced by a signal at ~3.3–3.5 ppm given by the quaternized ammonium groups in QDPMAEMA (data not shown).

Table 1
Molecular weights and dispersities of the well-defined α-N_3-PDMAEMA.

α-N_3-PDMAEMA copolymers	Theoretical M_n (g mol^{-1})	M_n NMR (g mol^{-1})	$\bar{M}_n$ SEC (g mol^{-1})	Đ
8C1 8C7	8 000	6 500	10 000	1.1
6C1 6C7	6 000	5 500	8 500	1.1
4C1 4C7	4 000	4 000	6 000	1.2
2C1 2C7	2 000	3 000	5 000	1.2

3.3. Immobilization of QPDMAEMAs on PLA surfaces

In accordance with the strategy described in Scheme 1, the next step consisted in immobilizing QPDMAEMAs on the PLA clickable surface by the CuAAC click reaction. This "grafting onto" strategy by heterogeneous reaction has been widely used in the recent past to functionalize various substrates, but not on PLA. In contrast to the "grafting from" technique, which can provide precise control over grafting density, the "grafting onto" technique is known to yield less uniform and substantially lower grafting densities. However, its major advantages lie in the possibility of preparing polymers with a variety of architectures and grafting them using simple and mild conditions, which is advantageous when dealing with degradable polyester surfaces [35].

In our previous work, we demonstrated the feasibility of transposing this approach to PLA, which is known to be sensitive towards degradation depending on the reaction conditions. Using the same conditions, the CuAAC reaction was carried out in aqueous medium using copper sulfate and sodium ascorbate as a catalytic system and α-N_3QPDMAEMAs were reacted for 2 days before treatment. Grafting was confirmed by XPS analysis. Compared to neat PLA (Supplementary Information Fig. S4), an XPS survey scan of the PLA-*g*-QPDMAEMA (8C1) showed one additional peak corresponding to N 1*s* at 398 eV (Supplementary Information Fig. S5a). High-resolution XPS in the C 1*s* and N 1*s* regions also confirmed the covalent grafting of QPDMAEMA (Supplementary Information Fig. S5a and b), together with partial quaternization of the PDMAEMA chains (85–90%) calculated by NMR analysis. Previous studies have shown that the presence of tertiary amines impacts the antibacterial activity of PDMAEMA without this being detrimental due to the high degree of protonation ($\alpha \approx 0.7$) at physiological pH (DMAEMA p$K_a \approx 8.4$) [36–38]. It has also been reported that combining amino and ammonium groups may help reduce hemotoxicity while maintaining potent antibacterial activity [37]. The chemical composition of the PLA-*g*-QPDMAEMA surface, calculated from the XPS analyses, consisted of C 1*s* 65.3%, O 1*s* 33.8% and N 1*s* 0.9%. Compared to the surface chemical compositions of PLA and QPDMAEMA, these values roughly correspond to 10% coverage of

the PLA surface by the covalently grafted PDMAEMA. An AFM characterization was also made of the PLA-*g*-QPDMAEMA surface (Fig. 1c). Compared to the propargylated surface, the PLA-*g*-QPDMAEMA surface showed greater roughness (24 nm vs. 14 nm). This increase is likely due to QPDMAEMA clusters on the surface. Such clusters (~25 nm) have been described by Huang et al. on glass surfaces when using a "grafting onto" technique [35]. In the study described herein, the clusters did not appear to have any sharp contours because of the pre-existing roughness of the propargylated PLA surface. Further insight into QPDMAEMA grafting and clustering was obtained by analyzing AFM height map profiles (Fig. 2). In comparison to the propargylated PLA, the PLA surface grafted with QPDMAEMA showed far more segregated areas with a profile composed of plateaux and valleys corresponding to maximal amplitude of 75 nm. This pattern and the 25 nm amplitude increase probably result from the presence of QPDMAEMA clusters on the PLA surface.

3.4. Anti-adherence activity of the modified PLA surfaces

Bacterial infection and proliferation on the surface of implantable materials relies on a four-step mechanism that starts with bacterial attachment to the surface. This is followed by bacterial accumulation in multiple layers mediated by microbial surface components recognizing adhesive matrix molecules. Third comes biofilm maturation by the accumulation of extracellular polymeric substances that results in the appearance of sessile bacteria that are not susceptible to conventional antibiotics. Finally, cells detach from the biofilm in a planktonic state. This causes the dispersal of small bacterial colonies and results in a more general and pronounced infection [7]. The strategy described here, based on the use of non-specific antibacterial PQAs, should help prevent bacterial adhesion (i) by increasing the anti-adherence character of the PLA surface as a result of the PQA conformation and increasing the surface hydrophilicity; and (ii) by killing the few bacteria that do manage to adhere to the surface.

Previous studies have demonstrated that QPDMAEMAs have antibacterial effects both in solution and on the surface of biomaterials [35,36,38–41]. In the study described herein, we focused on assessing the effect of MW and alkylating agent on QPDMAEMA antibacterial activity, as both these parameters are critical [29,35,37–39,42]. Indeed, PQA binding to the bacterial cytoplasmic membrane and their diffusion through the cell wall are believed to be linked both to electrostatic interactions (MW) and hydrophobic interactions (alkyl chain length). Thus, an optimal range of alkyl chain lengths and MWs exists for the antibacterial action of these polymers which may differ depending on the substrate/PQA couple.

The anti-adherence efficiency of the modified PLA surfaces was first evaluated for *E. coli* (Gram-negative bacillus) and *S. aureus* (Gram-positive coccus), which are among the most representative bacterial strains responsible for nosocomial infections. Fig. 3 illustrates the effect of QPDMAEMA MW and alkylating agent on anti-adherence activity. The proposed combinatorial screening

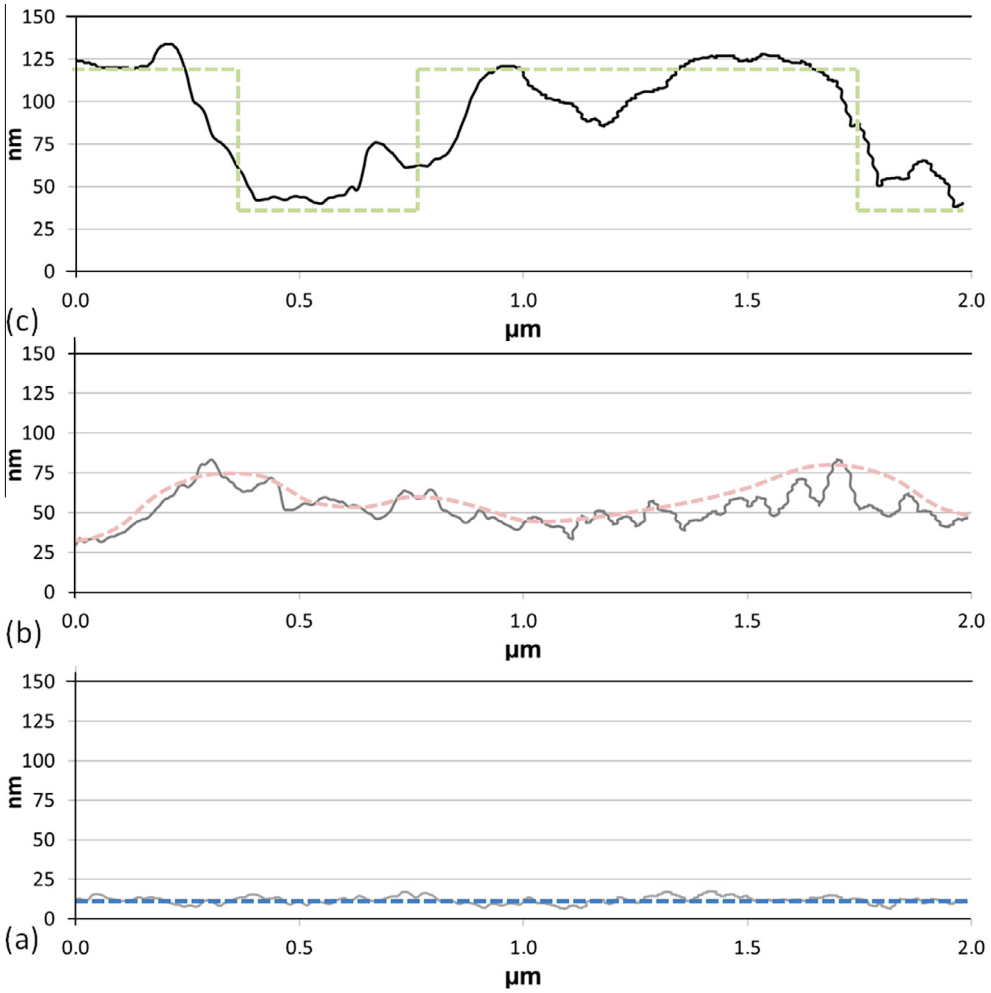

Fig. 2. Typical height profile analysis of AFM images. PLA surface (a) before modification, (b) after propargylation and (c) after functionalization with QPDMAEMA (8C7).

highlighted two main results. First, anti-adherence efficiency was greater with the longer C7 alkylating agent than the C1 alkylating agent, and this for all QPDMAEMAs, which is in agreement with previous studies indicating that an optimum is obtained for alkyl chains at around C8 [38,42,43]. More precisely, whereas QPDMAEMAs quaternized by C1 showed low antibacterial activity up to 10 0000 g mol^{-1}, all QPDMAEMAs quaternized by C7 were active. Secondly, the anti-adherence effect increased with QPDMAEMA MW, with as few as one residual living bacterium per million being present on the surface modified with 10 0000 g mol^{-1} and C7 QPDMAEMAs (8C7). Use of modified strain *E. coli gfp+* confirmed these results, showing decreasing bacterial adherence with increasing m, and even no adherent bacteria visible for the 8C7 polymer (Supplementary Information Fig. S6). Considering that grafting density was the same for all the polymers, these results contradict the findings of Huang et al. who did not report any effect of MW on the bactericidal activity of PQAs for degree of polymerization (DP) ranging from 50 to 200 [35]. An explanation for this might lie in the lower DP, ranging from 30 to 60, used in the present studies. In fact, a parabolic relation with MW has been described for various polycations in solution, and this is strongly influenced by the nature of the polycation [29,30]. It is therefore reasonable to assume that the lower DP used in the present studies remains on the steepest part of this parabola and explains the observed major impact of MW variations. A number of factors have been proposed to explain the decrease in activity at high MWs, e.g. a decreased capacity to penetrate through outer membranes and cell walls [26]. In addition, when considering surface modifications, another explanation may lie in different possible conformations of the polymer chains on the surface, and in different grafting densities. In fact, Huang et al. used copolymers, not homopolymers, for anchoring purposes and this may have given rise to conformational differences between the two systems, e.g. partial collapse onto the surface, thus explaining the differences observed in terms

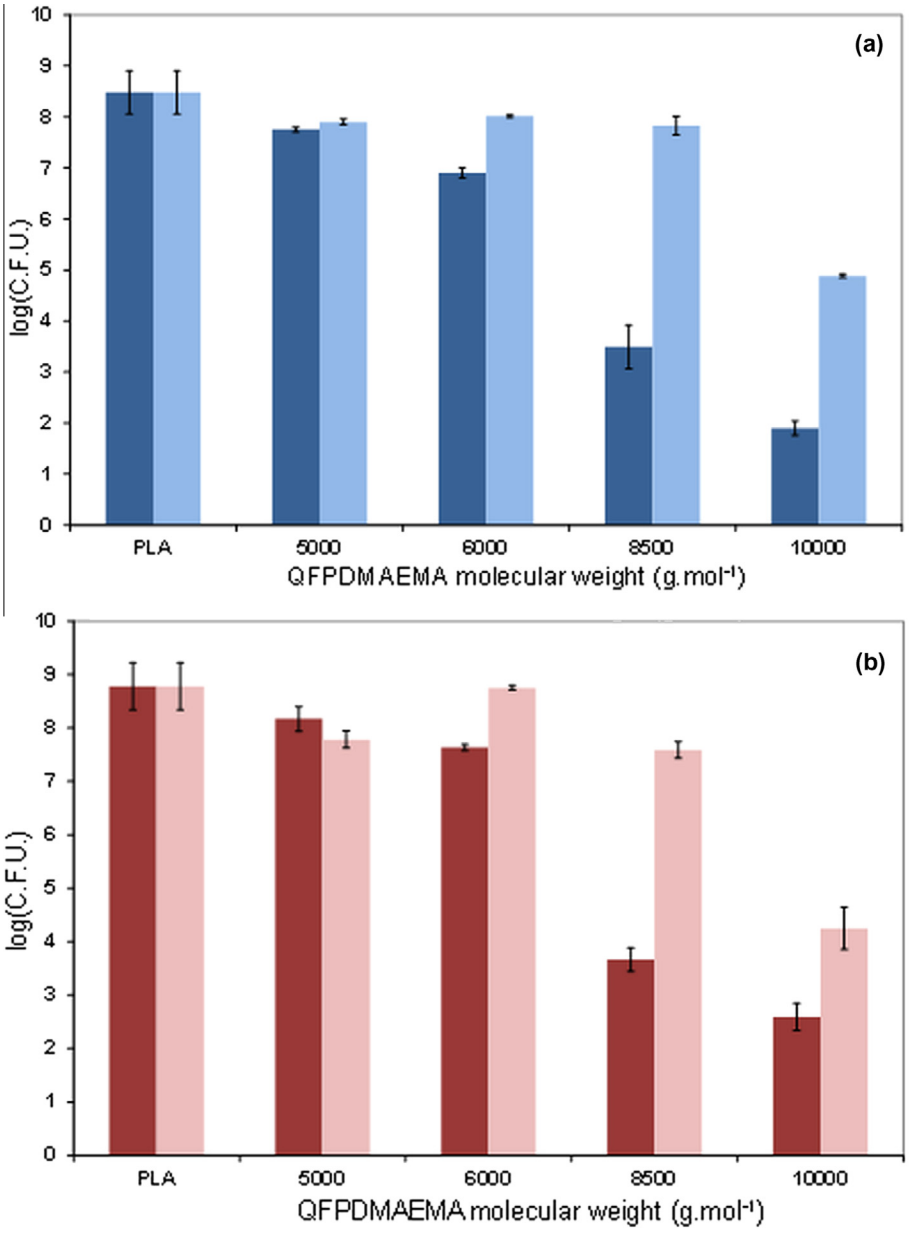

Fig. 3. Number of adherent bacteria as a function of the QPDMAEMA molecular weight and alkylating agent: (a) *E. coli* (C7 dark blue bars, C1 light blue bars) and (b) *S. aureus* (C7 dark red bars, C1 light red bars) (data are expressed as means ± SD and correspond to measurements in triplicate).

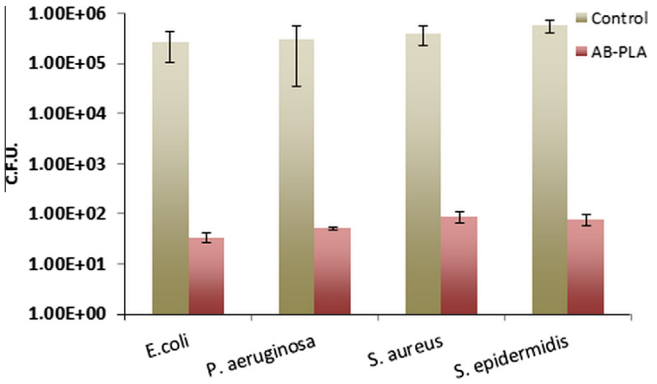

Fig. 4. Antibacterial activity of 8C7 modified PLA surface against four bacterial strains: *E. coli, P. aeruginosa, S. aureus* and *S. epidermidis* (data are expressed as means ± SD and correspond to measurements in triplicate).

of MW impact (Supplementary Information Scheme S2). In the study described herein, it should be noted that the proposed PLA surfaces showed very potent antibacterial activity, with reduction factors (ASTM E 2149–01) superior to 99.999% for the best surfaces vs. 97% in the cited study (Supplementary Information Table S2) [35]. Interestingly, similarly high efficiencies were also found against other Gram-negative (*P. aeruginosa*) and Gram-positive (*S. epidermidis*) isolates (Fig. 4). This confirmed the non-specific antibacterial activity of QPDMAEMAs which, in the MW range concerned, are able to diffuse through the looser cell wall of Gram-positive bacteria as well as the more challenging outer membrane and cell wall of Gram-negative bacteria.

3.5. Bactericidal and antibiofilm activities of the modified PLA surfaces

Having demonstrated that the modified PLA plates are potently anti-adherent, we further investigated the antibacterial activity of these surfaces by conducting a Live/Dead assay. As for the adherence tests, the plates were placed in contact with bacterial cultures for 1 h before being incubated for 24 h. They were then immersed in Live/Dead BacLight® solution which stains bacteria with intact membranes green, and those with ruptured membranes red. As shown in Fig. 5, the modified PLA plates not only decreased the number of adherent bacteria, but also killed the few adherent ones.

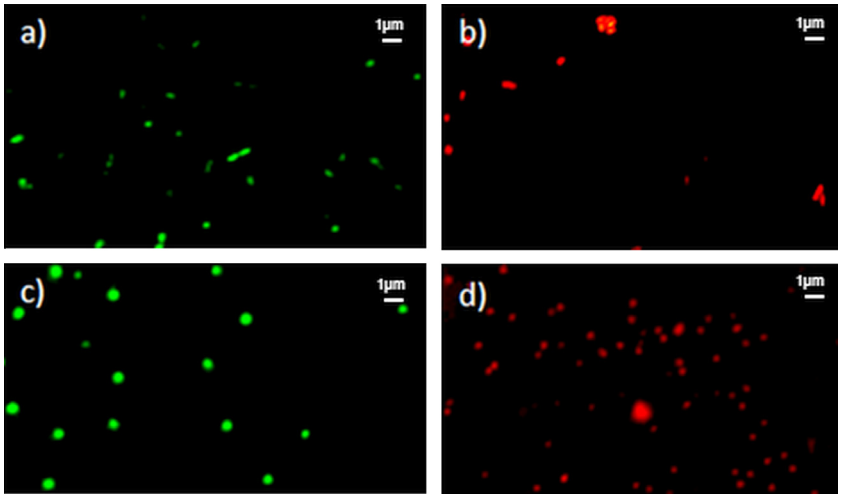

Fig. 5. Live/Dead assay: (a) *E. coli* control plate, (b) *E. coli* 8C7 modified plate, (c) *S. epidermidis* control plate, (d) *S. epidermidis* 8C7 modified plate.

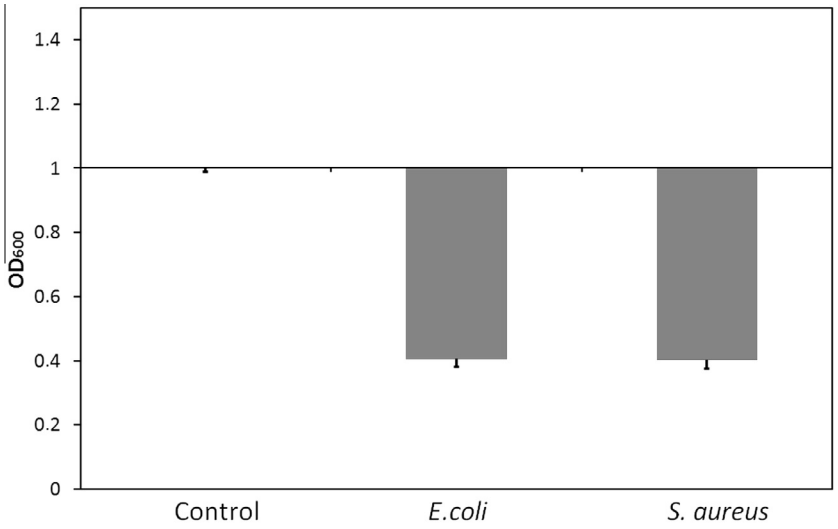

Fig. 6. Quantification of the *E. coli* and *S. aureus* biofilms on 8C7 PLA plates after 16 h by crystal violet staining and measurement of the released stained bacteria at OD_{600} (the results are expressed relative to the biofilm on control plates, data are expressed as means ± SD and correspond to measurements in triplicate).

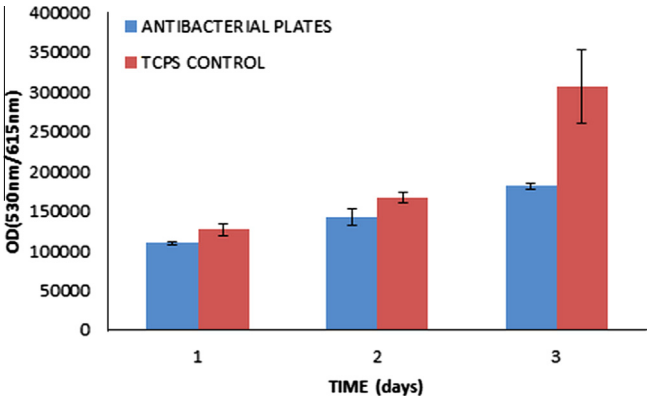

Fig. 7. L929 proliferation on 8C7 modified PLA surfaces (blue bars) compared to TCPS control (red bars) (data are expressed as means ± SD and correspond to measurements in triplicate).

And the red staining with the 8C7 modified plate (Fig. 5b and d) confirmed that grafted QPDMAEMA chains kill bacteria by damaging and rupturing their membrane. Again, this cell lysis mechanism was found to be effective against both Gram-negative and Gram-positive strains, with similar results found for the four test strains (results shown only for *E. coli* and *S. epidermidis*). Finally, biofilm formation was evaluated on the most promising antibacterial plate (8C7) by luminometry and fluorescence microscopy. Marked anti-biofilm activity was found with the 8C7 modified PLA on both test bacterial strains (*E. coli* and *S. aureus*). As shown in Fig. 6, the total number of bacteria in the biofilm formed after 16 h of incubation decreased greatly, as demonstrated by the 60% decrease in OD_{600} compared to the control surface. However, given the very potent anti-adherence activity and bactericidal activity of the antibacterial PLA plates, this presence of residual biofilm may seem surprising. First, however, it should be noted that the static conditions used in this study may have influenced biofilm formation as it has been reported that antibacterial activity may in some cases be regenerated by washing [44]. Therefore, the physiological environment of in vivo implants may help to continuously wash away dead bacteria and thus maintain optimal activity. Secondly, it should be recalled that this study was conducted under drastic conditions, with particularly high concentrations of bacteria present in the test suspension ($\sim 1 \times 10^5$ CFU ml^{-1}). Such concentrations are at the upper end of the range for biofilm studies where concentrations one-tenth of these are often used [45,46]. It is very unlikely that such locally high concentrations of bacteria would be reached under clinical conditions during the implantation process since for typical infections around 10^2 CFUs are observed and up to 10^3 CFUs for urinary tract infections [47–49]. Given these remarks, the potent antibiofilm activity of the modified PLA surfaces, in addition to their marked anti-adherence activity, confirms that these antibacterial biomaterials are of great promise and should be further considered for in vivo evaluation.

3.6. Cytocompatibility of the modified PLA surfaces

PQAs have a number of advantages over low MW QAs, including enhanced antibacterial activity, reduced residual toxicity, low tissue irritation tendencies in mammals, increased efficiency and selectivity, and prolonged lifecycle [50]. Given their final potential application as antibacterial implants, we were interested in evaluating the cytocompatibility of our antibacterial PLA surfaces that in addition to exerting potent antibacterial effects should also not be toxic to the tissues surrounding the implantation site, and should not hinder cell proliferation. The 8C7-grafted PLA surface, which showed the most potent antibacterial activity, was chosen as a control surface for cytocompatibility tests conducted on the L-929 fibroblast cell line, as recommended by international and European standards [51]. L929 fibroblasts adhered and proliferated on the antibacterial PLA surface, showing a 1.7-fold increase after 3 days (Fig. 7). Cell proliferation was slower than with the TCPS control but nevertheless significant with relative proliferation of about 60%. Modification of the PLA surface with QPDMAEMA therefore provided highly efficient antibacterial activity with no toxic effects on cells.

4. Conclusion

Non-leaching antibacterial PLA surfaces were prepared by the "grafting onto" technique using well-defined QPDMAEMAs. This was achieved by combining mild anionic activation of the PLA surface, ensuring no degradation of the polyester, with a highly efficient click reaction for QPDMAEMA grafting under mild, heterogeneous conditions. The effect of PQA MW (5000–10000 g mol^{-1}) and alkylating agent (C1–C7) on overall antibacterial activity was assessed. The most potent antibacterial activity of the tested range was obtained by modifying the PLA surface with 10 000 g mol^{-1} and C7 quaternized QPDMAEMAs. This surface was highly efficient against the four bacterial strains tested, including Gram-negative and Gram-positive bacteria, by decreasing their adherence and killing the few bacteria that did manage to adhere. In addition, biofilm formation was markedly reduced, with 60% fewer bacteria. Finally, antibacterial PLA surfaces were found to be cytocompatible and should be considered for future investigations in the field of implantable degradable biomaterials.

Acknowledgments

The authors wish to thank the French Ministry of Education and Research for S.E.H.'s fellowship, the Erasmus program for B.P.'s fellowship, Valérie Flaud for the XPS analyses, Michel Ramona for the AFM analyses and Sylvie Hunger and Cedric Paniagua for the NMR characterizations.

Appendix A. Figures with essential colour discrimination

Certain figures in this article, particularly Figures 1–5 and 7, are difficult to interpret in black and white. The full colour images can be found in the on-line version, at http://dx.doi.org/10.1016/j.actbio.2013.04.018.

Appendix B. Supplementary data

Supplementary data associated with this article can be found, in the online version, at http://dx.doi.org/10.1016/j.actbio.2013.04.018.

References

[1] Kingshott P, Andersson G, McArthur SL, Griesser HJ. Surface modification and chemical surface analysis of biomaterials. Curr Opin Chem Biol 2011;15:667–76.
[2] Birch C. The use of prosthetics in pelvic reconstructive surgery. Best Pract Res Clin Obstet 2005;19:979–91.
[3] Goldstein H. Selecting the right mesh. Hernia 1999;3:23–6.
[4] Rokkanen PU, Böstman O, Hirvensalo E, Mäkelä EA, Partio EK, Pätiälä H, et al. Bioabsorbable fixation in orthopaedic surgery and traumatology. Biomaterials 2000;21:2607–13.
[5] (a) Campoccia D, Montanaro L, Arciola CR. The significance of infection related to orthopedic devices and issues of antibiotic resistance. Biomaterials 2006;27:2331–9;
(b) Danese PN. Antibiofilm approaches: prevention of catheter colonization. Chem Biol 2002;9:873–80.

[6] Bliziotis IA, Kasiakou SK, Kapaskelis AM, Falagas ME. Mesh-related infection after hernia repair: case report of an emerging type of foreign-body related infection. Infection 2006;34:46–8.
[7] Arciola CR, Campoccia D, Speziale P, Montanaro L, Costerton JW. Biofilm formation in Staphylococcus implant infections. A review of molecular mechanisms and implications for biofilm-resistant materials. Biomaterials 2012;33:5967–82.
[8] Costerton JW, Stewart PS, Greenberg EP. Bacterial biofilms: a common cause of persistent infections. Science 1999;284:1318–22.
[9] Lewis K. Persister cells, dormancy and infectious disease. Nat Rev Microbiol 2007;5:48–56.
[10] Guillaume O, Lavigne JP, Lefranc O, Nottelet B, Coudane J, Garric X. New antibiotic-eluting mesh used for soft tissue reinforcement. Acta Biomater 2011;7:3390–7.
[11] Lepretre S, Chai F, Hornez JC, Vermet G, Neut C, Descamps M, et al. Prolonged local antibiotics delivery from hydroxyapatite functionalised with cyclodextrin polymers. Biomaterials 2009;30:6086–93.
[12] Shameli K, Bin Ahmad M, Yunus WMZW, Ibrahim NA, Rahman RA, Jokar M, et al. Silver/poly (lactic acid) nanocomposites: preparation, characterization, and antibacterial activity. Int J Nanomed 2010;5:573–9.
[13] Teo EY, Ong SY, Chong MSK, Zhang ZY, Lu J, Moochhala S, et al. Polycaprolactone-based fused deposition modeled mesh for delivery of antibacterial agents to infected wounds. Biomaterials 2011;32:279–87.
[14] Xu XL, Zhong W, Zhou SF, Trajtman A, Alfa M. Electrospun PEG-PLA nanofibrous membrane for sustained release of hydrophilic antibiotics. J Appl Polym Sci 2010;118:588–95.
[15] Bazaka K, Jacob MV, Crawford RJ, Ivanova EP. Plasma-assisted surface modification of organic biopolymers to prevent bacterial attachment. Acta Biomater 2011;7:2015–28.
[16] Desmet T, Morent R, De Geyter N, Leys C, Schacht E, Dubruel P. Nonthermal plasma technology as a versatile strategy for polymeric biomaterials surface modification: a review. Biomacromolecules 2009;10:2351–78.
[17] Ishihara K, Kyomoto M. Photo-induced functionalization on biomaterials surfaces. J Photopolym Sci Technol 2010;23:161–6.
[18] Kiss E, Kutnyanszky E, Bertoti I. Modification of poly(lactic/glycolic acid) surface by chemical attachment of poly(ethylene glycol). Langmuir 2010;26:1440–4.
[19] Wang SG, Cui WJ, Bei JZ. Bulk and surface modifications of polylactide. Anal Bioanal Chem 2005;381:547–56.
[20] Xu FJ, Wang ZH, Yang WT. Surface functionalization of polycaprolactone films via surface-initiated atom transfer radical polymerization for covalently coupling cell-adhesive biomolecules. Biomaterials 2010;31:3139–47.
[21] Xu FJ, Yang XC, Li CY, Yang WT. Functionalized polylactide film surfaces via surface-initiated ATRP. Macromolecules 2011;44:2371–7.
[22] Nottelet B, Coudane J, Vert M. Synthesis of an X-ray opaque biodegradable copolyester by chemical modification of poly (epsilon-caprolactone). Biomaterials 2006;27:4948–54.
[23] Nottelet B, El Ghzaoui A, Coudane J, Vert M. Novel amphiphilic poly(epsilon-caprolactone)-g-poly(L-lysine) degradable copolymers. Biomacromolecules 2007;8:2594–601.
[24] Nottelet B, Vert M, Coudane J. Novel amphiphilic degradable poly(epsilon-caprolactone)-graft-poly (4-vinyl pyridine), poly (epsilon-caprolactone)-graft-poly(dimethylaminoethyl methacrylate) and water-soluble derivatives. Macromol Rapid Commun 2008;29:743–50.
[25] El Habnouni S, Darcos V, Garric X, Lavigne JP, Nottelet B, Coudane J. Mild methodology for the versatile chemical modification of polylactide surfaces: original combination of anionic and click chemistry for biomedical applications. Adv Funct Mater 2011;21:3321–30.
[26] Ikeda T, Yamaguchi H, Tazuke S. New polymeric biocides—synthesis and antibacterial activities of polycations with pendant biguanide groups. Antimicrob Agents Chemother 1984;26:139–44.
[27] Kugler R, Bouloussa O, Rondelez F. Evidence of a charge-density threshold for optimum efficiency of biocidal cationic surfaces. Microbiol-Sgm 2005;151:1341–8.
[28] Milovic NM, Wang J, Lewis K, Klibanov AM. Immobilized N-alkylated polyethylenimine avidly kills bacteria by rupturing cell membranes with no resistance developed. Biotechnol Bioeng 2005;90:715–22.
[29] Kenawy ER, Worley SD, Broughton R. The chemistry and applications of antimicrobial polymers: a state-of-the-art review. Biomacromolecules 2007;8:1359–84.
[30] Timofeeva L, Kleshcheva N. Antimicrobial polymers: mechanism of action, factors of activity, and applications. Appl Microbiol Biotechnol 2011;89:475–92.
[31] Gutierrez-Villarreal MH, Ulloa-Hinojosa MG, Gaona-Lozano JG. Surface functionalization of poly(lactic acid) film by UV-photografting of N-vinylpyrrolidone. J Appl Polym Sci 2008;110:163–9.
[32] Agut W, Taton D, Lecommandoux S. A versatile synthetic approach to polypeptide based rod-coil block copolymers by click chemistry. Macromolecules 2007;40:5653–61.
[33] Balazs DJ, Triandafillu K, Wood P, Chevolot Y, van Delden C, Harms H, et al. Inhibition of bacterial adhesion on PVC endotracheal tubes by RF-oxygen glow discharge, sodium hydroxide and silver nitrate treatments. Biomaterials 2004;25:2139–51.
[34] Zhang X, Xia JH, Matyjaszewski K. Controlled/"living" radical polymerization of 2-(dimethylamino)ethyl methacrylate. Macromolecules 1998;31:5167–9.
[35] Huang JY, Koepsel RR, Murata H, Wu W, Lee SB, Kowalewski T, et al. Nonleaching antibacterial glass surfaces via "grafting onto": the effect of the number of quaternary ammonium groups on biocidal activity. Langmuir 2008;24:6785–95.
[36] Lenoir S, Pagnoulle C, Detrembleur C, Galleni M, Jerome R. New antibacterial cationic surfactants prepared by atom transfer radical polymerization. J Polym Sci Pol Chem 2006;44:1214–24.
[37] Palermo EF, Kuroda K. Chemical structure of cationic groups in amphiphilic polymethacrylates modulates the antimicrobial and hemolytic activities. Biomacromolecules 2009;10:1416–28.
[38] Roy D, Knapp JS, Guthrie JT, Perrier S. Antibacterial cellulose fiber via RAFT surface graft polymerization. Biomacromolecules 2008;9:91–9.
[39] Murata H, Koepsel RR, Matyjaszewski K, Russell AJ. Permanent, non-leaching antibacterial surfaces—2: how high density cationic surfaces kill bacterial cells. Biomaterials 2007;28:4870–9.
[40] Wang HW, Wang L, Zhang PC, Yuan L, Yu QA, Chen H. High antibacterial efficiency of pDMAEMA modified silicon nanowire arrays. Colloid Surf B 2011;83:355–9.
[41] Yao F, Fu GD, Zhao JP, Kang ET, Neoh KG. Antibacterial effect of surface-functionalized polypropylene hollow fiber membrane from surface-initiated atom transfer radical polymerization. J Membr Sci 2008;319:149–57.
[42] Gilbert P, Altaae A. Antimicrobial activity of some alkyltrimethylammonium bromides. Lett Appl Microbiol 1985;1:101–4.
[43] Riva R, Lussis P, Lenoir S, Jerome C, Jerome R, Lecomte P. Contribution of "click chemistry" to the synthesis of antimicrobial aliphatic copolyester. Polymer 2008;49:2023–8.
[44] Kanazawa A, Ikeda T, Endo T. Polymeric phosphonium salts as a novel class of cationic biocides. 6. Antibacterial activity of fibers surface-treated with phosphonium salts containing trimethoxysilane groups. J Appl Polym Sci 1994;52:641–7.
[45] Ferreira FA, Souza RR, Bonelli RR, Americo MA, Fracalanzza SEL, Figueiredo AMS. Comparison of in vitro and in vivo systems to study ica-independent Staphylococcus aureus biofilms. J Microbiol Methods 2012;88:393–8.
[46] Niska JA, Shahbazian JH, Ramos RI, Pribaz JR, Billi F, Francis KP, et al. Daptomycin and tigecycline have broader effective dose ranges than vancomycin as prophylaxis against a *Staphylococcus aureus* surgical implant infection in mice. Antimicrob Agents Chemother 2012;56:2590–7.
[47] Mishra B, Srivastava S, Singh K, Pandey A, Agarwal J. Symptom-based diagnosis of urinary tract infection in women: are we over-prescribing antibiotics? Int J Clin Pract 2012;66:493–8.
[48] Ronco E, Denys P, Bernede-Bauduin C, Laffont I, Martel P, Salomon J, et al. Diagnostic criteria of urinary tract infection in male patients with spinal cord injury. Neurorehabil Neural Repair 2011;25:351–8.
[49] Walsh CA, Moore KH. Overactive bladder in women: does low-count bacteriuria matter? A review. Neurourol Urodynam 2011;30:32–7.
[50] Gabrielska J, Sarapuk J, Przestalski S, Wroclaw P. Investigations of new bis-ammonium salts with potential biological application. Tenside Surf Det 1994;31:296–8.
[51] AFNOR. Biological evaluation of medical devices—Part 5: Tests for in vitro cytotoxicity. 2009;ISO 10993-5:2009.